Numerical study of localization in the two-state Landau level

K. Minakuchi and S. Hikami
Department of Pure and Applied Sciences, University of Tokyo,
Meguro-ku, Komaba 3-8-1, Tokyo 153, Japan
(Received 7 August 1995; revised manuscript received 26 December 1995)

A two-state model of the lowest Landau level, which includes only interband scattering, is investigated. The localization properties are studied numerically based on the iterative Green function method. The singularity of the density of states at the band center is examined in addition to the study of the localization length exponent. Other extended states located away from the band center are also discussed.

I. INTRODUCTION

Although the localized-delocalized (LD) transition in the quantum Hall effect (QHE) has been studied extensively by numerical simulations,[1] there is no satisfactory theoretical explanation for the critical behavior of the LD transiton.

The usual theoretical analyses neglect the spin dependence of the Landau level. Here we consider a spin-degenerate case: when Zeeman splitting is very small, the energy of the Landau level becomes degenerate. Under an impurity potential, an electron scatters between different spin states. Recently Lee and Chalker[2] and Wang, Lee, and Wen[3] investigated this spin scattering in the QHE by introducing a two-channel network model, and they obtained the same value of the localization exponent as in the spinless case, although the location of the extended states become different from the band center.

Assuming that impurity scattering occurs only between different spin states, and neglecting the scattering within the same spin state, Hikami, Shirai, and Wegner[4] obtained a finite longitudinal conductivity at the band center in the lowest Landau level (LLL). They suggested that the density of states (DOS) of this two-state LLL model is singular at the band center ($E=0$) by a $1/N$ expansion. However, the true nature of the singularity remains unsolved because there is a crossover from the semicircle law near the band center. This particular model may correspond to the limit of a strong spin-orbit case: at each scattering, the electron spin has to flip to the opposite state. Hanna, Arovas, Mullen, and Girvin[5] have also tried to analyze this two-state model by calculating the Thouless number. Lee[6] has argued that there appear three extended states, one at the band center and two other states.

The main purpose of this paper is to investigate further this two-state LLL model numerically, focusing especially on the DOS and the localization exponent. To evaluate the DOS, we employ the iterative Green function method (MacKinnon-Kramer method),[7] which is a suitable method for large system size and for the region near the band center.

This paper is organized as follows. In Sec. II we present the model and explain the iterative Green function method. Sections III and IV are dedicated to numerical results for the DOS and the localization exponent, respectively. The effect of Zeeman splitting is investigated in Sec. V. Discussions and some comments are presented in Sec. VI.

II. MODEL AND METHOD

The two-state random scattering problem in the quantum Hall regime is expressed by the following Hamiltonian:

$$H=\frac{1}{2m}(p+eA)^2+\begin{pmatrix}0 & h(r)\\ \overline{h(r)} & 0\end{pmatrix}. \tag{1}$$

The 2×2 matrix represents two spin states. Since we consider only the subspace of the LLL, the first term becomes trivial. $h(r)$ is a random spin-impurity scattering potential and $\overline{h(r)}$ is its complex conjugate. We impose the following correlation for the random potential $h(r)$:

$$\langle h(r)\rangle=\langle\overline{h(r)}\rangle=0, \tag{2}$$

$$\langle h(r)\overline{h(r')}\rangle=w\,\delta(r-r'), \tag{3}$$

where $\langle\ \rangle$ denotes the ensemble average. The distribution is Gaussian white noise. The matrix in Eq. (1) has no diagonal elements: there is no impurity scattering within the same spin state.

In order to analyze this Hamiltonian numerically, we employ MacKinnon and Kramer's iterative Green function method.[7] This method works also for the study of the DOS of a finite system.[8] Details of the calculation by this method may be seen in the literature[1,9] and here we present its brief description. Let us consider an $L_x\times L_y$ strip geometry ($L_x\gg L_y$). We impose a periodic boundary condition in the y direction and use the Landau gauge: $A=(-By,0)$. For a pure system, the LLL eigenfunctions are

$$u_{k_n}(x,y)=\frac{1}{\sqrt{L_y}}e^{-ik_n y}\frac{1}{\sqrt{\sqrt{\pi}l_c}}e^{-(x-k_n l_c^2)^2/2l_c^2}, \tag{4}$$

which are labeled with $k_n=2\pi n/L_y$ ($n=1,2,\ldots,L_xL_y/2\pi l_c^2$). l_c is the magnetic length $\sqrt{eB/m}$ and we take $\sqrt{2\pi}l_c$ as the unit length hereafter. We have also spin indices denoted by A and B (spin up and down) for the present two-state model.

Introducing real $h_{x,y}$ by $h(r)=h_x(r)+ih_y(r)$, and $\overline{h(r)}=h_x(r)-ih_y(r)$, the random potential correlation Eqs. (2) and (3) becomes

$$\langle h_{x,y}(r)\rangle=0, \tag{5}$$

$$\langle h_x(r)h_x(r')\rangle=\langle h_y(r)h_y(r')\rangle=\frac{w}{2}\delta(r-r'). \tag{6}$$

We realize $h_{x,y}$ putting δ-potential scatterers randomly in the system (the typical density of the scatterers is four per unit area $2\pi l_c^2$).

Since the functions Eq. (4) become exponentially small at large $(x-k_n l_c^2)$, the matrix elements $(k_n,k_{n'})$ can be neglected for $|k_n l_c^2-k_{n'} l_c^2|\gg l_c$. We therefore introduce a cutoff length $l_{\rm cutoff}$, which is equal to $2\sqrt{2\pi}l_c$. We divide the system into cells in the x direction and the length of each cell is chosen as $l_{\rm cutoff}$. Then the Hamiltonian becomes

$$H=\sum_{I=1,N_{\rm cell}}\{|I\rangle\mathbf{H}_{I,I}\langle I|+|I\rangle\mathbf{H}_{I,I+1}\langle I+1|+|I+1\rangle\mathbf{H}_{I+1,I}\langle I|\}, \tag{7}$$

where we denote states in the cell by ket vectors. We define a Green function by

$$G_{I,J}^{(N)}(E)=\left\langle I\left|\frac{1}{E-H^{(N)}}\right|J\right\rangle, \tag{8}$$

where $H^{(N)}$ is a part of the Hamiltonian composed of the first N cells. This Green function can be solved iteratively by the following recursion formula:

$$G_{1,N+1}^{(N+1)}=G_{1,N}^{(N)}\mathbf{H}_{N,N+1}G_{N+1,N+1}^{(N+1)}, \tag{9}$$

$$G_{N+1,N+1}^{(N+1)}=[E-\mathbf{H}_{N+1,N+1}-\mathbf{H}_{N+1,N}G_{N,N}^{(N)}\mathbf{H}_{N,N+1}]^{-1}. \tag{10}$$

The localization length of a finite system, with M width in the y direction $(M=L_y/\sqrt{2\pi}l_c)$, is given by

$$\lambda_M^{-1}(E)=-\frac{1}{2N_{\rm cell}l_{\rm cutoff}}\ln{\rm Tr}|G_{1,N_{\rm cell}}^{(N_{\rm cell})}(E)|^2. \tag{11}$$

The DOS can be obtained by a similar recursion formula for ${\rm Tr}\Sigma_{J=1,N}G_{J,J}^{(N)}(E+i\epsilon)$. The details may be found in Ref. 8.

Finally, we mention the normalization of energy and the DOS in our calculation. We measure energy by the unit energy $\Gamma=2\sqrt{w}$ and denote the normalized energy by E_n. The DOS is normalized by the integration over the whole energy. This leads to

$$\int \Gamma\rho(\Gamma E_n)dE_n=1. \tag{12}$$

Therefore we define the normalized DOS by $\rho_n(E_n)\equiv\Gamma\rho(\Gamma E_n)$.

The DOS, the imaginary part of the Green function, is represented in the small $\epsilon\to0$ limit as

$$-\frac{1}{\pi}{\rm Im}\frac{1}{E+i\epsilon-H}=\frac{1}{\pi}\frac{\epsilon}{(E-H)^2+\epsilon^2}[\to\delta(E-H)\ \text{ as }\epsilon\to0]. \tag{13}$$

The approximation of the DOS with a finite ϵ corresponds to an average (integration) of the true DOS over the finite width ϵ.

III. DENSITY OF STATES

By the iterative Green function method, we obtain the DOS and the localization length of a finite system. The behavior of the DOS is shown in Fig. 1(a). A singularity at the band center is observed and it is consistent with the result of the perturbative approach by the $1/N$ expansion.[4] In addition to the singular band-center behavior, there is a hump around $E_n\sim0.4$. It is quite different behavior from the usual one-state (spinless) LLL case, which was exactly solved by Wegner.[10] To see its band-center singularity more clearly, we make a ρ_n–$(\ln E_n)^2$ plot in the energy range [0.005, 0.1] [Fig. 1(b)]. Its curve is almost straight. This means that the perturbative result $\rho_n(E_n)\sim(\ln|E_n|)^2$ is quite good in the region $0.005<|E_n|<0.1$, i.e., about 1/10 of the bandwidth. It is interesting to clarify whether the band-center density $\rho_n(0)$ is divergent or not. Our numerical approach, however, cannot determine this point clearly due to the finite range integration described in the previous section. Here, we calculate the DOS at $E_n=0,0.001,0.01$ with several system sizes and several energy resolutions ϵ. The results are summarized in Table I. The value of $\rho_n(0)$ slightly increases when the system size M is larger or when ϵ is smaller. This seems to imply the weak divergence of the infinite $(M\to\infty)$ system. On the other hand, the dependence of the DOS at $E_n=0.001$ and 0.01 on M and ϵ is very small. So it is considered that the $(\ln|E_n|)^2$ behavior near the band center [Fig. 1(b)] is unchanged for larger M.

When the system width is narrow (typically $M<2$), $\rho_n(E_n)$ near the band center becomes very small [Fig. 1(c)]. It seems that if we set $M\to0$, $\rho_n(0)$ goes to 0. This can be understood as follows. For the case of $M<1$, $|k_n l_c^2-k_{n'} l_c^2|$ for different k_n and $k_{n'}$ is much larger than l_c. So, from Eq. (4), the matrix elements between different k_n and $k_{n'}$ are negligible. Therefore the Hamiltonian becomes

$$H=\begin{pmatrix}\begin{matrix}0 & v_1\\ \overline{v_1} & 0\end{matrix} & & & \\ & \begin{matrix}0 & v_2\\ \overline{v_2} & 0\end{matrix} & & \\ & & \ddots & \\ & & & 0\end{pmatrix} \tag{14}$$

with basis $\{|k_1A\rangle,|k_1B\rangle,|k_2A\rangle,|k_2B\rangle,\dots\}$ and each $v_j(j=1,2,\dots)$ follows the same distribution independently. Since h_x and h_y are independent, ${\rm Re}(v_j)$ and ${\rm Im}(v_j)$ must be independent variables. We assume that the distribution of ${\rm Re}(v_j)$ and ${\rm Im}(v_j)$ is Gaussian $P_e(\alpha)$:

$$P_e(\alpha)\propto e^{-a\alpha^2}. \tag{15}$$

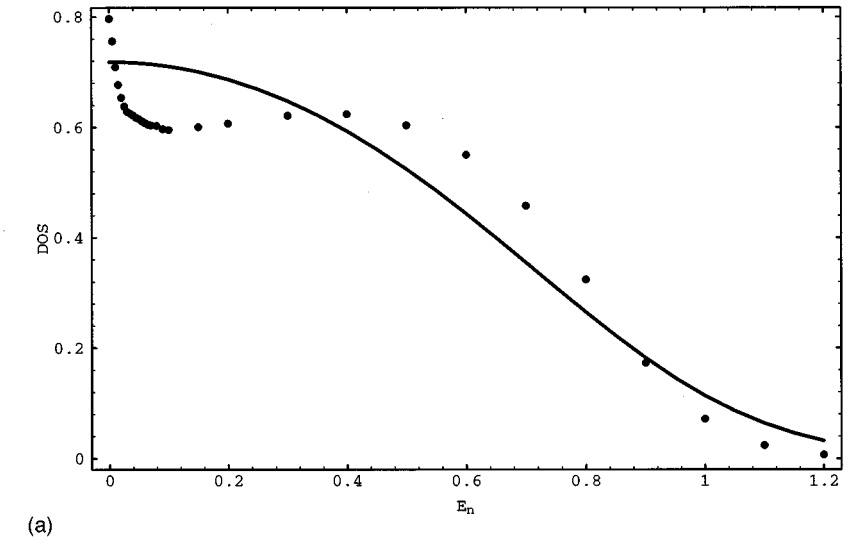

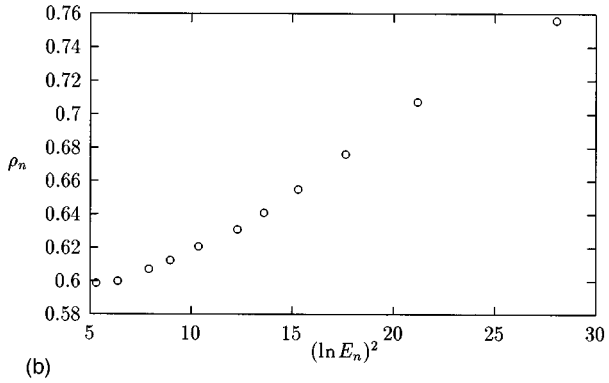

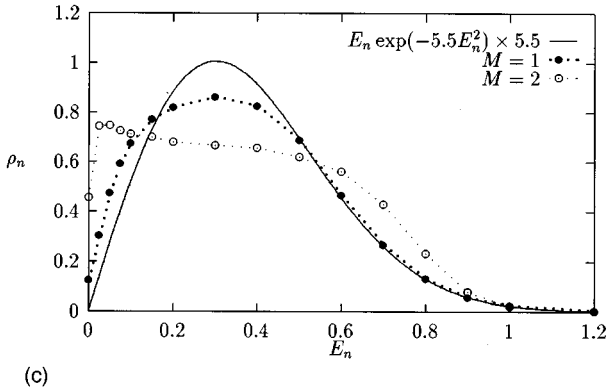

FIG. 1. (a) The DOS for a two-state LLL model with interspin (interband) disorder. System size is $M=12$ and $N_{\text{cell}}=5\times10^4$, which means $L_y=12\sqrt{2\pi}l_c$, $L_x=10^5 2\sqrt{2\pi}l_c$ (l_c is the magnetic length), and we choose $\epsilon=5\times10^{-3}$. Exact solution for the usual one-state LLL model is a solid line. (b) The DOS near the band center: ρ_n-$(\ln E_n)^2$ plot. (c) The DOS for the narrow limit ($M=1,2$). The solid line is Eq. (18) with $a=5.5$ for the best fit.

Since the Hamiltonian Eq. (14) is already block diagonalized and each 2×2 block is statisticaly independent, it is enough to take out one block. The eigenvalues λ satisfy the equation

$$\begin{vmatrix} -\lambda & v \\ \overline{v} & -\lambda \end{vmatrix} = 0. \tag{16}$$

So we get the eigenvalue $\lambda=\pm|v|$. Then the eigenvalue distribution $P(\lambda)$, i.e., the density of states, is given by

$$P(\lambda)=\int_{-\infty}^{\infty} dv_R dv_I [\,\delta(\lambda-|v|)+\delta(\lambda+|v|)\,]P_e(v_R)P_e(v_I). \tag{17}$$

TABLE I. The DOS near the band center (averaged over five samples). Upper: $E_n=0$; middle: $E_n=0.001$; lower: $E_n=0.01$. Typical system length $N_{\rm cell}$ is 1×10^4.

ϵ	M 8	16	32
	1.04 ± 0.05	1.13 ± 0.02	1.16 ± 0.02
5×10^{-4}	1.00 ± 0.02	0.97 ± 0.02	0.97 ± 0.01
	0.72 ± 0.04	0.69 ± 0.01	0.68 ± 0.01
	1.06 ± 0.06	1.38 ± 0.07	1.59 ± 0.04
1×10^{-4}	1.03 ± 0.08	0.97 ± 0.03	0.96 ± 0.01
	0.73 ± 0.06	0.67 ± 0.03	0.68 ± 0.02
	0.89 ± 0.10	1.52 ± 0.14	1.83 ± 0.03
5×10^{-5}	0.99 ± 0.04	0.95 ± 0.04	0.97 ± 0.03
	0.71 ± 0.03	0.68 ± 0.04	0.68 ± 0.04

In polar coordinates for positive λ [of course, $P(-\lambda)=P(\lambda)$],

$$P(\lambda)\propto 2\pi\int_0^\infty r dr\,\delta(\lambda-r)e^{-ar^2}$$
$$\propto|\lambda|e^{-a\lambda^2}. \tag{18}$$

This suggests that the DOS vanishes at $E_n=0$ and increases linearly.

A comparison between Eq. (18) and the numerical results for $M=1,2$ is shown in Fig. 1(c). The $M=1$ case appears to be well approximated by Eq. (18). Note that vanishing $\rho_n(0)$ is due to the measure of the random variables, i.e., the presence of two independent disorders (h_x,h_y). It does not depend on whether the distribution P_e is Gaussian. Therefore we can recognize it as a kind of level repulsion.

This explains also the existence of a hump in Fig. 1(a). It is known that pure off-diagonal disorder causes a singular DOS at the band center. The one-dimensional tight-binding model with off-diagonal disorder, which was studied in Ref. 11, is one example. Our DOS in Fig. 1(a) can be regarded as a superposition of a band-center enhancement caused by off-diagonal disorder and Ee^{-aE^2}-type behavior that is seen in the narrow limit.

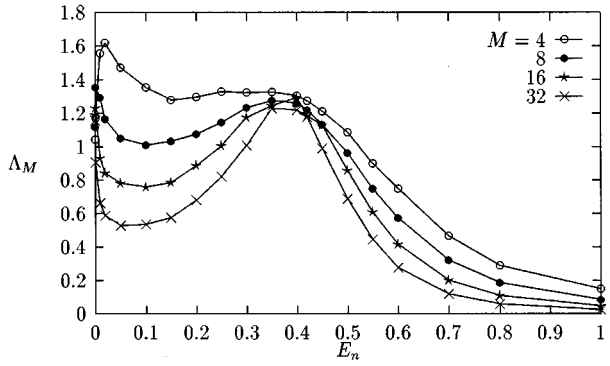

FIG. 2. The renormarized localization length for several E_n. Length of the system $N_{\rm cell}$ is 3×10^4.

TABLE II. System width dependence of the renormalized localization length Λ_M near the band center.

M	8	16	32
$\Lambda_M(E_n=0.0001)$	1.11 ± 0.02	1.14 ± 0.03	1.14 ± 0.06

IV. LOCALIZATION EXPONENT

Next, we discuss the localization property. An overall profile of the renormalized localization length $\Lambda_M(E_n)=\lambda_M(E)/M$ is presented in Fig. 2. (λ_M is the localization length of a finite strip with width M.) At first sight, we recognize the existence of three extended states at $E_n=0,\pm0.365$. We analyze these data with the one-parameter scaling relation

$$\Lambda_M(E_n)=f(\xi(E_n)/M) \tag{19}$$

and determine the localization length $\xi(E_n)$.

As can be seen in Fig. 2, the critical region of the LD transition at the band center is very narrow and the finite size effect influences these data strongly. For a small-width system, the peak location of Λ_M is not $E_n=0$. When the system width M becomes larger, the peak location shifts toward $E_n=0$. On the other hand, Λ_M at $E_n=0.0001$, which is the closest to the band center in the present study, is almost independent of width M (see Table II). This implies scale invariance and hence the existence of an extended state at the band center in spite of the small system sizes. For the odd behavior of the peak of Λ_M, application of the standard

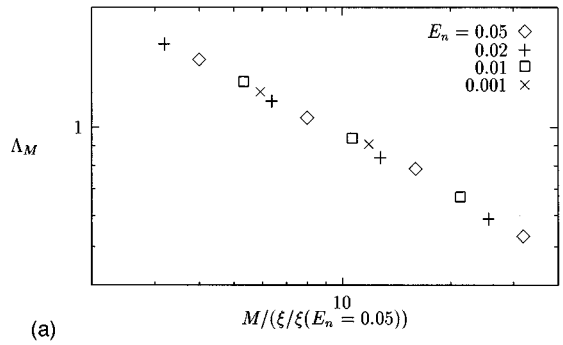

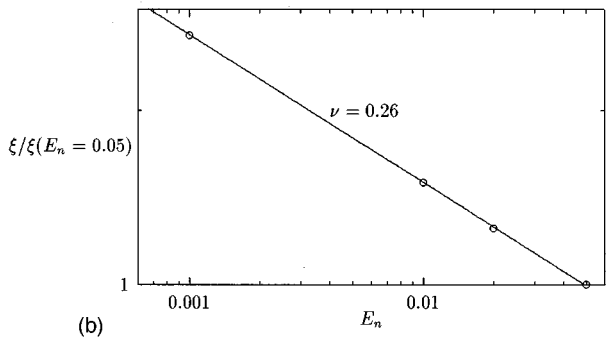

FIG. 3. (a) The renormalized localization length vs $\xi(E_n)/M$ for the LD transition at $E_n=0$. (b) ξ vs E_n.

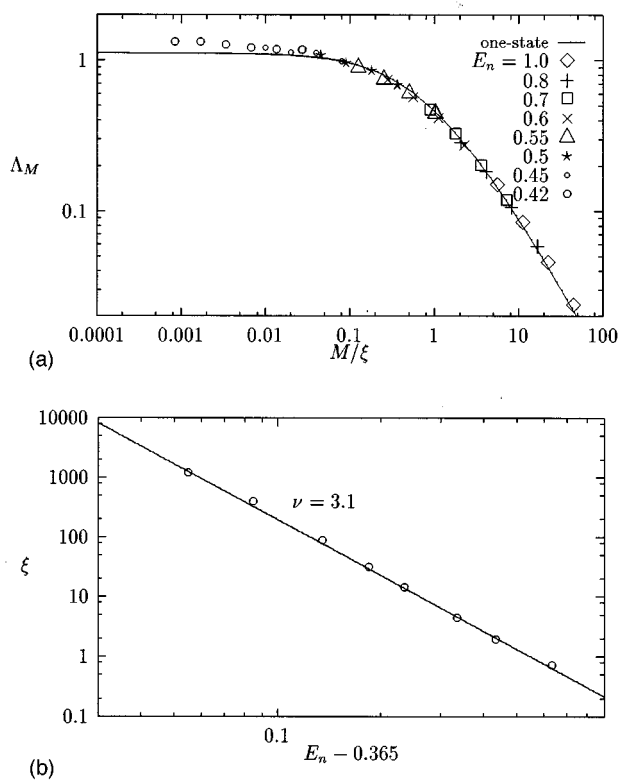

FIG. 4. (a) The renormalized localization length vs $\xi(E_n)/M$ for the LD transition at $E_n=0.365$. The solid line is the scaling curve of the one-state LLL case (calculated by the same method). (b) ξ vs $E_n-0.365$.

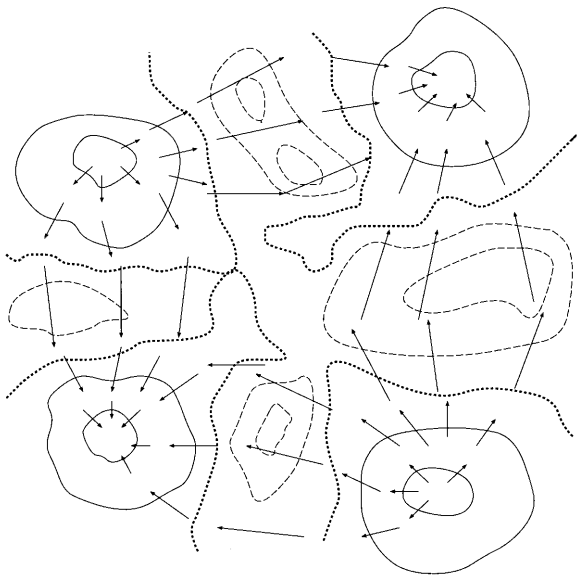

FIG. 5. The illustration of a random potential (h_x,h_y). The random potential is expressed by a two-dimensional vector field (arrows). Solid lines, dashed lines, and dotted lines are equi-$|h|$ lines, which correspond to small $|h|$, large $|h|$, and critical $|h|(=|h|_c)$, respectively.

one-parameter scaling relation Eq. (19) is inappropriate. Nevertheless, when we try it only with the data which lie in the region of the right side of the peak, we obtain the exponent $\nu=0.26\pm0.02$ [Fig. 3(a) and 3(b)]. This value violates the Chayes *et al.* inequality,[12] which gives $\nu\geqslant 2/d$ (where d is the spatial dimension). Of course this value is a tentative one and if larger systems are accessed, it may be possible that the exponent ν will change into a value which satisfies the Chayes *et al.* inequality. Anyway, we cannot go further in the present study.

We analyze the LD transition near $E_n=0.365$ with the one-parameter scaling relation Eq. (19). From the data of the large-$|E_n|$ region, we obtain the scaling curve in [Fig. 4(a)], the critical energy $E_{c1}=0.365$, and the localization exponent $\nu=3.1\pm0.2$ [Fig.4(b)]. The data in the region [0.1,0.35] are strongly affected by the crossover between the two LD transitions, hence we do not apply the scaling relation to the data in this region. [The shapes of Λ_M-E_n curves in narrow systems are highly asymmetric around E_{c1}, but in the widest system of the present study ($M=32$), the curve is almost symmetric around E_{c1}.] In Fig. 4(a), we also depict the scaling curve of the LD transition of the one-state LLL with short-range scattering. Although the exponent $\nu=3.1$ does not agree with the usual one-state LLL value 2.3, the two scaling curves are quite similar. The limiting value $\lim_{M\to\infty}\Lambda_M$ of the two-state model is about 1.2, close to that of the one-state model, 1.13. These features remind us of the LD transition of the one-state higher Landau levels. Several studies reported nonuniversal behavior of the localization length exponent in higher Landau levels, that is, dependence on the range of scatterers. A recent study of Huckestein,[1,13] however, reveals that there exists an irrelevant operator in the case of higher Landau levels and that the seemingly nonuniversal behavior is due to the finite size effect of the irrelevant field. We consider that this is also the case for the LD transition at E_{c1} of the two-state LLL and, therefore, that the universality class is the same as that of the one-state LLL.

The existence of three extended states can be understood following Lee's semiclassical argument.[6] We consider smooth disorder, i.e., the length scale of variation of the disorder potential is much larger than the magnetic length. (In our numerical study, this is not the case, but we believe the qualitative features are not unchanged.) But now the disorder has two components $(h_x(x,y),h_y(x,y))$. An example of the disorder potential is seen in Fig. 5. There are some vortices, which correspond to $h_x=h_y=0$. In the semiclassical treatment, an electron's guiding center moves along equienergy lines. Since we restrict the Hilbert space to the lowest Landau level, the electron energy is given by the second term of Eq. (1), i.e., $E=\pm|h|$ $[|h|=\sqrt{(h_x^2+h_y^2)}]$. This energy can be regarded as Zeeman coupling to a random pseudomagnetic field (h_x,h_y), and its sign corresponds to spin parallel or antiparallel to this local pseudomagnetic field. Therefore equienergy lines are equal to equi-$|h|$ lines. So a low-$|E|$ electron moves with a vortex inside, and a high-$|E|$ electron moves with a vortex outside. At an intermediate energy, an electron's motion will spread over the whole system because there is a critical value $|h|_c$ where the equi-$|h|$ lines percolate (see Fig. 5). This picture leads to the extended state at $E_n=\pm E_{c1}$. In this way, the LD transition at $E_n=\pm E_{c1}$ is essentially the percolation of a random field (h_x,h_y). This is the same story for the usual one-state (spinless) model which is described in the Chalker-Coddington network model.[14] Therefore it is suggested that the univer-

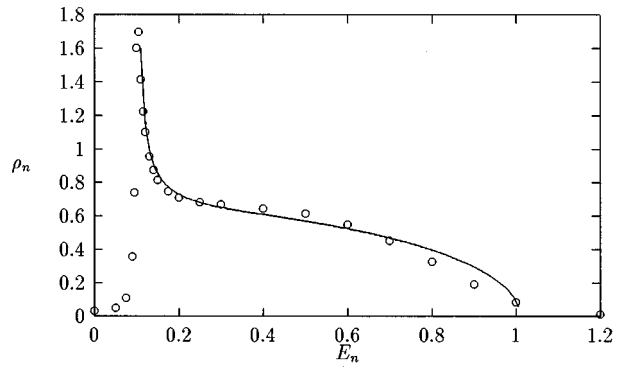

FIG. 6. The DOS in the case of Zeeman splitting $\Delta=0.1$ ($M=12$, $N_{\rm cell}=20\,000$, and $\epsilon=5\times10^{-3}$). Equation (24) is expressed by a solid line.

sality class of the LD transition at $E_n=E_{c1}$ is the same as in the one-state case. But how about the extended state at $E=0$? In this picture, $E=0$ corresponds to $|h|=0$, i.e., a vortex core. Following Lee's argument, each vortex has an exact $E=0$ state and its energy spectrum is symmetric around $E=0$. So each exact $E=0$ state can hybridize and spread over the whole system and it leads to the extended state at $E=0$. But this picture cannot tell us about its localization exponent.

V. EFFECT OF ZEEMAN SPLITTING

So far, the two states A and B (spin up and down states) are completely degenerate. In this section we put an energy difference 2Δ between the A and B states. This can be achieved by adding the following term to Eq. (1):

$$\begin{pmatrix} -\Delta & 0 \\ 0 & \Delta \end{pmatrix}. \tag{20}$$

The effect on the DOS is easily understood within the lowest-order perturbation of disorder strength w. The Dyson equation becomes up to order w

$$G_A=G_{0A}+wG_AG_BG_{0A}, \quad G_B=G_{0B}+wG_BG_AG_{0B}. \tag{21}$$

Here, we denote the renormalized Green function of A and B state electrons by G_A and G_B and the bare one by G_{0A} and G_{0B}, i.e., $G_{0A}=1/(E+\Delta)$ and $G_{0B}=1/(E-\Delta)$. The solution is

$$G_A=\frac{1-\sqrt{1-4wG_{0A}G_{0B}}}{2wG_{0B}}, \quad G_B=\frac{1-\sqrt{1-4wG_{0A}G_{0B}}}{2wG_{0A}}. \tag{22}$$

The DOS is given by

$$\rho(E)=-\frac{1}{2\pi}\mathrm{Im}[G_A(E)+G_B(E)]. \tag{23}$$

After some normalization, we get

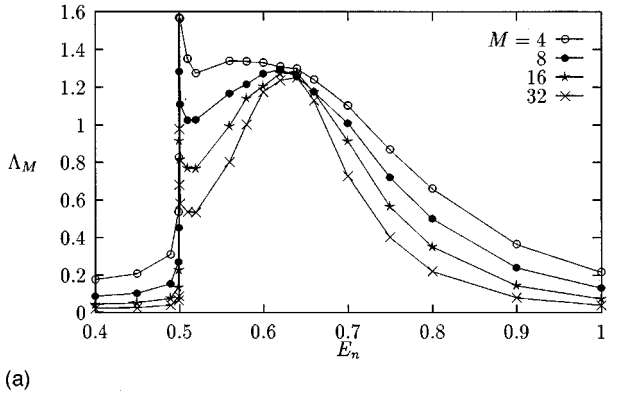

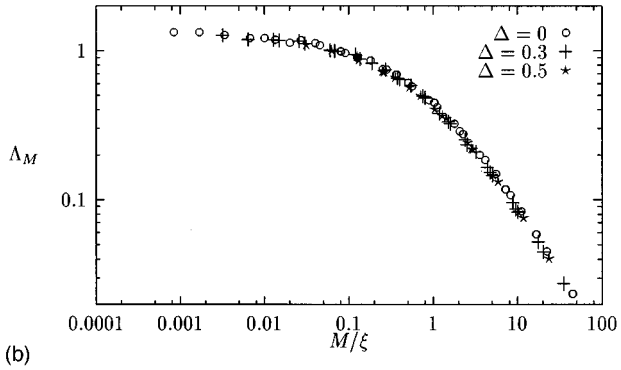

FIG. 7. (a) The renormarized localization length for several E_n in the $\Delta=0.5$ case. (b) The scaling curve for $\Delta=0$, 0.3, and 0.5.

$$\rho_n(E_n)=\frac{2E_n}{\pi}\sqrt{\frac{(E_e-E_n)(E_e+E_n)}{(E_n-\Delta)(E_n+\Delta)}}, \tag{24}$$

where $E_e=\sqrt{\Delta^2+1}$. The energy gap in $[-\Delta,\Delta]$ is *never* filled with off-diagonal disorder, and the DOS at $E_n=\pm\Delta$ is more enhanced than in the $\Delta=0$ case; in fact, it diverges as $|E_n\pm\Delta|^{-1/2}$ (but is still normalizable). The next order term of the perturbational series can be carried out as in Ref. 4, but it only leads to weaker divergence, as $(\ln|E_n\pm\Delta|)^2$.

Numerical results are depicted in Fig. 6 with the lowest-order perturbation results Eq. (24). Their coincidence is good. The numerical results indicate a small tail of the DOS in the region $[-\Delta,\Delta]$. But this is artificial, arising from the integration nature of the method, described in Sec. II, and divergence of $E_n=\Delta$.

We study the localization length exponent for $\Delta=0.3,0.5$. For example, the renormalized localization

TABLE III. E_{c1} and the localization exponents for $\Delta=0$, 0.3, and 0.5.

Δ	0	0.3	0.5
E_{c1}	0.365	0.48	0.62
ν	3.1 ± 0.2	2.8 ± 0.2	3.0 ± 0.2
$\sqrt{\Delta^2+[E_{c1}(0)]^2}$	0.365	0.472	0.619

length vs E_n for $\Delta=0.5$ is presented in Fig. 7(a). We can see the existence of the extended states at $E_n=\pm 0.62\equiv\pm E_{c1}(\Delta=0.5)$. From the scaling plot for $E_n=E_{c1}$, we obtain the exponent $\nu=3.0\pm 0.2$, which is almost the same value as in the zero Zeeman splitting case, and its scaling curve is in good coincidence with the zero Zeeman one [Fig. 7(b)]. We conclude that Zeeman splitting does not change the universality class of the LD transition at $E_n=E_{c1}$. We summarize the critical energy E_{c1} and its exponent ν for $\Delta=0$, 0.3, 0.5 in Table III. But, unfortunately, the behavior near $E_n=\Delta$ is obscure, and we cannot determine whether the $E_n=\pm\Delta$ state is localized or extended.

Those properties can be understood with the semiclassical picture again. In the semiclassical limit (a smooth random potential case), an electron energy can be expressed as

$$E=\sqrt{\Delta^2+|h|^2}. \tag{25}$$

This makes a band gap in $[-\Delta,\Delta]$ apparently. Denoting the distribution function of $|h|$ by $R(|h|)$, the DOS is given by

$$\rho_\Delta(E)dE=R(|h|)d|h|. \tag{26}$$

Of course, the DOS for $\Delta=0$ is $\rho_{\Delta=0}(E)=R(E)$. For the Zeeman splitting case, we get

$$\rho_\Delta(E)=\frac{E}{\sqrt{E^2-\Delta^2}}\rho_{\Delta=0}(E) \tag{27}$$

from the energy dispersion relation Eq. (25). So the DOS diverges as $|E\pm\Delta|^{-1/2}$ and a gap in $[-\Delta,\Delta]$ is not filled. These results are consistent with the previous perturbative calculation, Eq. (24). The shift of the extended state energy E_{c1} is also understood. This extended state is associated with the percolation of $|h|$, so the critical value $|h|_c$ is not changed from the $\Delta=0$ case. This shows that the extended state energy $E_{c1}(\Delta)$ is equal to $\sqrt{\Delta^2+|h|_c^2}=\sqrt{\Delta^2+[E_{c1}(0)]^2}$. This picture is well supported by our numerical simulation, as shown in Table III.

VI. SUMMARY AND DISCUSSIONS

In this paper we investigate the two-state LLL model numerically. The density of states has a singularity, which is well approxiamated by $(\ln|E_n|)^2$, at the band center, and the localization length diverges at three energies, i.e., $E_n=0,\pm E_{c1}$. The obtained value of the localization exponent is 3.1 ± 0.2 for $E_n=\pm E_{c1}$ and 0.26 ± 0.02 for $E_n=0$, but the latter is not conclusive in this study because of the narrow critical region and small system size. The transitions at $E_n=\pm E_{c1}$ are considered to belong to the conventional quantum Hall universality class. This behavior is consistent with the semiclassical argument for a smooth disorder potential. In spite of the present study, several questions remain open. We do not have complete understanding of the band-center singularity yet. Another question is the Hall conductivity σ_{xy}. In Ref. 6, Lee conjectures that σ_{xy} does not jump at the band center.

Throughout this paper, we do not consider the scattering within the same spin state. When we introduce this intraspin scattering in addition, we think that the extended state at $E_n=0$ will be destroyed, but that the extended states at $E_n=\pm E_{c1}$ will survive. This $\pm E_{c1}$ state corresponds to the delocalized states in the two-channel network model.[2,3] So we think that our results for the two-state model do not contradict the two-channel network model.

The singular behavior at the band center originates in the reflection symmetry of the Hamiltonian Eq. (1):

$$\sigma_z H\sigma_z=-H. \tag{28}$$

From this symmetry, a state of energy E has to be accompanied by a state of energy $-E$. Of course, the $E=0$ state is special. Recently, Hikami and Zee[15] analyzed a lattice of a complex random matrix, which has the same reflection symmetry. This model also has the same singular density of states at the band center in $O(1/N^2)$, where N is the size of the random matrix. The reflection symmetry Eq. (28) also arises in some lattice systems.[16,17] Consider the two-dimensional tight-binding model on a square lattice with one-half of a flux quantum per plaquette. Since the square lattice is constructed of two sublattices A and B (bipartite structure), nearest-neighbor hopping attaches the A sublattice to the B sublattice. Introducing randomness to the nearest-neighbor hopping (due to randomness of a magnetic field), we obtain a two-state random scattering problem. This two-sublattice structure plays the role of the spin freedom of our two-state LLL model. (Of course, introducing random site energy in the lattice system corresponds to random scattering within the same spin state in our two-state model.) Ludwig *et al.*[17] studied this lattice model focusing on the $E=0$ state. After taking a continuum limit and mapping onto a $(2+1)$-dimensional Dirac fermion, they considered three types of disorder: random Dirac mass, random vector potential, and random scalar potential. Among these models, a random vector potential model has the reflection symmetry of Eq. (28), which is equivalent to chiral symmetry, and corresponds to random nearest-neighbor hopping in the original lattice system. This model in Ref. 17 has several properties which resemble our two-state LLL model. (i) At $E=0$, the DOS has a singularity. But the singularity depends on the strength of randomness. (ii) The longitudinal conductivity σ_{xx} at $E=0$ is finite. It has exactly the same value as in our two-state LLL model.[4,17] (iii) Its wave function at $E=0$ is extended. It is related to the index theorem.[6,16,17] It is of interest to investigate further the correspondence between our two-state model and a random vector potential model.

ACKNOWLEDGMENT

This work was supported in part by a Grant-in-Aid for Scientific Research by the Ministry of Education, Science and Culture.

[1] B. Huckestein, Rev. Mod. Phys. **67**, 357 (1995).
[2] D. K. K. Lee and J. T. Chalker, Phys. Rev. Lett. **72**, 1510 (1994).
[3] Z. Wang, D. H. Lee, and X. G. Wen, Phys. Rev. Lett. **72**, 2454 (1994).
[4] S. Hikami, M. Shirai, and F. Wegner, Nucl. Phys. **B408**, 415 (1993).
[5] C. B. Hanna, D. P. Arovas, K. Mullen, and S. M. Girvin, Phys. Rev. B **52**, 5221 (1995).
[6] D. K. K. Lee, Phys. Rev. B **50**, 7743 (1994).
[7] A. MacKinnon and B. Kramer, Phys. Rev. Lett. **47**, 1546 (1981); Z. Phys. B **53**, 1 (1983).
[8] A. MacKinnon, Z. Phys. B **59**, 385 (1985).
[9] D. Liu and S. Das Sarma, Phys. Rev. B **49**, 2677 (1994).
[10] F. Wegner, Z. Phys. B **51**, 279 (1983).
[11] G. Theodorou and M. H. Cohen, Phys. Rev. B **13**, 4597 (1976); T. P. Eggarter and R. Riedinger, *ibid.* **18**, 569 (1978).
[12] J. T. Chayes, L. Chayes, D. S. Fisher, and T. Spencer, Phys. Rev. Lett. **24**, 2999 (1986).
[13] B. Huckestein, Phys. Rev. Lett. **72**, 1080 (1994).
[14] J. T. Chalker and P. D. Coddington, J. Phys. C **21**, 2665 (1988).
[15] S. Hikami and A. Zee, Nucl. Phys. **B446**, 337 (1995).
[16] X. G. Wen and A. Zee, Nucl. Phys. **B316**, 641 (1989).
[17] A. W. W. Ludwig, M. P. A. Fisher, R. Shankar, and G. Grinstein, Phys. Rev. B **50**, 7526 (1994).